



Colour change and microstructure evolution of wet flowing paint when subject to shear

Y.-K. Chen^a, M. R. Mackley^{a,*}, T. S. B. Sayer^b

^aDepartment of Chemical Engineering, University of Cambridge, Cambridge CB2 3RA, UK

^bPPG Industries UK Ltd. Suffolk IP14 2AD, UK

Received 15 October 2002; received in revised form 20 January 2003; accepted 27 January 2003

Abstract

This paper reports an experimental method of measuring the colour change of wet paint when subject to a well-defined shear flow. Using a Multi-Pass Rheometer (MPR) and a modified colour spectrophotometer, the effect of shear on the colour changes of a red-pigmented paint were systematically studied. Substantial changes in paint colour during and after shear were observed for certain paint compositions. Additional direct optical observation on diluted paint samples strongly suggested that the key mechanism associated with the colour change was the state of pigment agglomerates during shear and the flocculation after shear. A model based on Mie scattering was developed to give a semi-quantitative prediction of the observed experimental trends.

© 2003 Elsevier Science Ltd. All rights reserved.

Keywords: Paint; Colour measurement; Microstructure; Aggregate dispersion; Scattering theory; Flow

1. Introduction

When certain types of pigmented paint are processed to form a coating surface, the resulting colour has been found to depend on the method of application. An example of this is the surface refinishing of cars. When the surface of a car is repainted with certain types of paint, even after using the same paint composition, the resulting colour may appear to be discernibly different if different spraying methods are used.

The colour properties of pigmented systems are determined by the chemical and crystallographic structure of the pigment itself, but the colour also depends on the particle size and the distribution of pigment in the medium in which it is applied (Volz, 1995). Günthert, Hauser, and Radtke (1989) have qualitatively summarised the effect of particle size on the colour properties of pigment suspensions such as colour strength, hiding power, transparency and gloss. Blakey (1989) compared the wet reflectance values of two types of titanium dioxide pigment dispersions. Kaluza (1982) discussed the effect of flocculation on the

colour property of paint using a “rub out test”. Although in this research quantitative results were presented to give evidence of the colour change effects, most of the previous research has focused on the colour behaviour of dry paint samples, and direct correlation between the particle size distribution and colour has not been made. Therefore, a key objective of this study was to develop a systematic, controlled experimental technique that enabled direct correlation between colour and pigment size.

The colour of a pigmented coating is the result of incident light interacting with pigment agglomerates and its surrounding media (Volz, 1995). Although the perception of colour involves a physical, chemical, physiological and even psychological understanding, its physical aspect can still be measured in the form of the reflectance of incident light. Fig. 1 illustrates the reflectance spectrum of a white and red tile. The spectrum of a white tile reflects the incident beam with high efficiency over the entire visible light wavelength spectrum, while that of a red reference paint sample only reflects the light partially, at a longer wavelength range. This type of reflectance measurement depends on factors such as the light source, measuring angle (see e.g. McDonald, 1997), and environmental illumination. As a result, a quantitative standardised colour measuring approach is required.

* Corresponding author. Tel.: +44-1223-334-777;
fax: +44-1223-334-796.

E-mail address: mrm1@cheng.cam.ac.uk (M. R. Mackley).

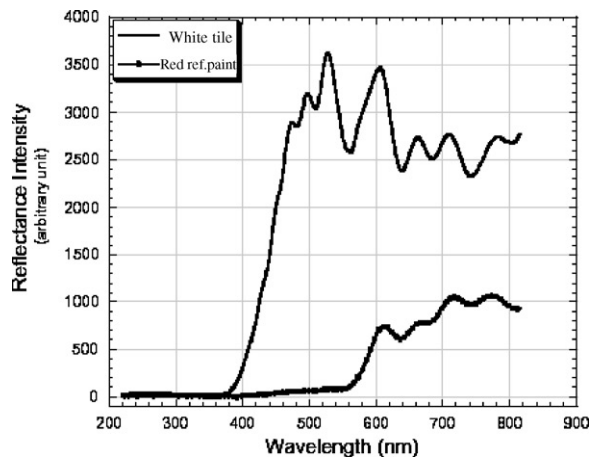


Fig. 1. Reflectance spectrum of a white tile and the red reference paint. The absolute value of the measurement depends on the spectral power distribution of the light source.

A colour system introduced by the CIE (International Commission of Illumination) was used in this research in order to quantitatively describe the colour of paint. (See for example Hunt, 2002 as a useful introduction to colour measurement.) The CIE successfully introduced a set of weighting functions, $\bar{x}(\lambda)$, $\bar{y}(\lambda)$, $\bar{z}(\lambda)$, from which a set of imaginary primaries, X , Y , Z can be obtained using the following equations:

$$\begin{aligned} X &= \int_{\lambda=400}^{700} \bar{x}_{\lambda}(\lambda) R_{\lambda} S_{\lambda} d\lambda, \\ Y &= \int_{\lambda=400}^{700} \bar{y}_{\lambda}(\lambda) R_{\lambda} S_{\lambda} d\lambda, \\ Z &= \int_{\lambda=400}^{700} \bar{z}_{\lambda}(\lambda) R_{\lambda} S_{\lambda} d\lambda. \end{aligned} \quad (1)$$

The term R_{λ} represents the experimental measured reflectance of the form shown in Fig. 1, and S_{λ} is the spectral power distribution of the light source, which depends on the incident illumination. Using this system, the imaginary primaries of any colour can be experimentally obtained when the S_{λ} of any particular incident source is known.

Amongst the many applications of the CIE system, a CIELAB colour difference formula (introduced in 1976) was widely adopted for the examination of pigmented coatings. This formula has the following form:

$$\begin{aligned} L^* &= 116 \left(\frac{Y}{Y_n} \right)^{1/3} - 16, \\ a^* &= 500 \left[\left(\frac{X}{X_n} \right)^{1/3} - \left(\frac{Y}{Y_n} \right)^{1/3} \right], \\ b^* &= 200 \left[\left(\frac{Y}{Y_n} \right)^{1/3} - \left(\frac{Z}{Z_n} \right)^{1/3} \right]. \end{aligned} \quad (2)$$

This system uses three spatial coordinates a^* (red-green axis), b^* (yellow-blue axis) and L^* (lightness axis) to define colour, and an overall colour difference dE between two sets of L^* , a^* , b^* values can be defined as the following equation (Wyszecki & Stiles, 1982).

$$\Delta E = [(\Delta L^*)^2 + (\Delta a^*)^2 + (\Delta b^*)^2]^{1/2}. \quad (3)$$

In Eq. (2), the X , Y , and Z are the imaginary primaries for any colour, and X_n , Y_n and Z_n are the imaginary primaries derived from the reflectance measurement of a perfect white surface. In order to obtain a reproducible colour measurement result, a reference calibration of the X_n , Y_n and Z_n before each experiment is crucial. In this work, the colour measurement was conducted using an X-Dap spectrophotometer (PolytekTM, Germany), and the calibration was performed using this spectrophotometer with respect to a reference white tile (Macbeth[®] Prom. No. 37183). The L^* , a^* , b^* values for this reference white tile are set to be (100, 0, 0) after calibration, and all other colours are measured accordingly.

The paint sample used was a commercial red automotive paint (ICI AUTOCOLOR P420-0409) manufactured by ICI. This paint used iron oxide (Fe_2O_3) as a primary pigment with acrylic resin and thinner for the continuous phase. The weight percentages of its key components are: pigment 13%, resin 67% and thinner 20%. This sample is designated the “red reference sample”. In addition, a millbase sample was also used, the composition of which is: pigment 47%, resin 37% and thinner 16% in weight percentage. This sample was prepared in the colour laboratory in ICI by simply mixing the three components in a bead-milling shaker for a period of time. The sample prepared with 120 min milling time was designated as MB120/47, while the other millbase sample with 30 min of milling time was symbolised as MB30/47.

2. Colour measurement using a multi-pass rheometer

The colour performance of paint has always been an area of importance for the paint manufacturer. However, difficulties arise where the surface condition of a wet paint sample can alter during measurement, due to the volatile nature of paint. Previous studies including Buttignol (1968) and Hotter, Sarofim, Dalzell, and Vasalos (1971) were limited to using dry paint films. In this research, in order to monitor the colour change of wet paint sample, an experimental device coupling a Multi-Pass Rheometer (MPR) and a colour measuring spectrophotometer was developed.

2.1. Colour measurement: experimental apparatus and experimental protocol

The Multi-Pass Rheometer is a piston-driven rheometer. Its main components include a central test section, and two hydraulically controlled pistons (Mackley, Marshall, & Smeulders, 1995). The central test section can be modified

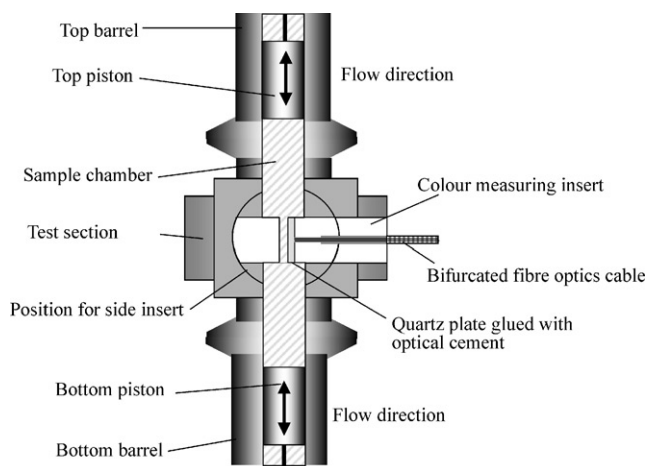


Fig. 2. Schematic diagram of the MPR with a modified centre section for colour measurement.

with different geometries such as a capillary or a slit in order to meet different experimental requirements. The test section of the MPR forms a fully enclosed chamber where test material can be completely contained, and hence it is suitable for handling volatile samples (Wee & Mackley, 1998). By moving both pistons at a controlled speed, the sample in the central section can be subjected to a shear deformation; the resulting differential pressure can be measured by two pressure transducers situated at either end of the test section. In the multi-pass mode of operation, both pistons move reciprocally at a controlled speed. If a very short interval between each stroke is used, the system can effectively apply “continuous shear” to a sample by the continuous reciprocal motion of the pistons.

In order to link the MPR with a colour measurement device, a newly designed central section was developed. The central section used a set of inserts to form a slit geometry. As shown in Fig. 2, a hole was drilled into the centre of one of the slit inserts, which allowed a bifurcated optical fibre bundle to be positioned at right angles to the slit face. This fibre optics cable was then connected to an X-Dap spectrophotometer for colour measurement. The tip of the fibre optic cable was positioned flush to the surface, and a quartz plate was then glued onto the surface with optical cement. The insert was placed perpendicular to the flow direction and the surface of the quartz was in contact with the test sample.

During colour measurement, light was transmitted along one set of the bifurcated bundles of fibre optics cable, through the quartz plate and into the liquid paint sample contained within the slit of the MPR (see Fig. 3). The back reflected light was then collected through the other fibre optic bundle and transmitted to the spectrophotometer. Data collection time for each colour spectrophotometer reading was set at 0.75 s. And the reflectance spectra accumulated within this 0.75 s time span was then converted into L^* , a^* and b^* colour values using a computer.

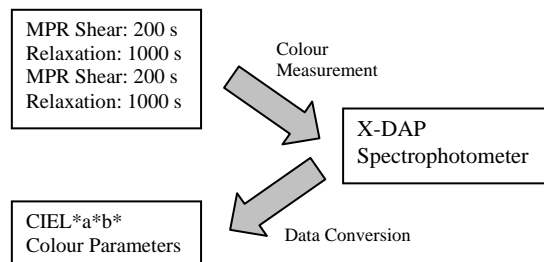


Fig. 3. Experimental protocol of the colour measurement experiment.

A series of experiments was carried out in which the paint was “continuously sheared” at a range of shear rates for a fixed time of 200 s. After the shearing period, the paint was held at rest for a further 1000 s, and the L^* , a^* and b^* colour measurement was continuously monitored throughout this 1200-s period. In this way, both steady shear L^* , a^* and b^* values and their relaxation behaviour after shear could be followed. For each shear condition, the whole experiment was then repeated in order to demonstrate reproducibility.

2.2. Results: red reference sample

Fig. 4 shows the colour measurement result of the red reference sample after both a low applied apparent wall shear rate of 13.8 s^{-1} and an apparent wall high shear rate of 3461.2 s^{-1} . The data shows the L^* , a^* and b^* values during the two shearing periods ($t = 0\text{--}200 \text{ s}$ and $t = 1200\text{--}1400 \text{ s}$). The relaxation of L^* , a^* and b^* after the shearing period is also shown. It was observed that the L^* , a^* and b^* values remained constant during the MPR shearing periods (0–200 s and 1200–1400 s). On the cessation of shear (the periods after 200 and after 1400 s), a reproducible and characteristic trend was observed. The L^* value showed an initial sudden drop with the cessation of shear followed by a slower decay. The a^* value increased slightly after shear and then decayed with a similar time dependence to the L^* value. The b^* value exhibited a slow decay throughout the relaxation period. The repeated sequence showed a strong correlation with the initial data. Hence, the experiment was reproducible and the material had a characteristic L^* , a^* and b^* value during shear for a given wall shear rate and also showed a characteristic relaxation process after shear.

Differences in the “steady state” values of L^* , a^* and b^* were compared with the partially relaxed state (defined as the value of L^* , a^* and b^* at $t = 1000 \text{ s}$ after shear cessation). This comparison is plotted in Fig. 5 as a function of apparent wall shear rate. When the wall shear rate increases, the values of dL^* and db^* increase, and so does the overall colour difference dE . The value of da^* , shows only a slightly increase.

2.3. Result: the red millbase samples

Colour measurement experiments were also performed on millbase samples. Fig. 6 shows the colour measurement

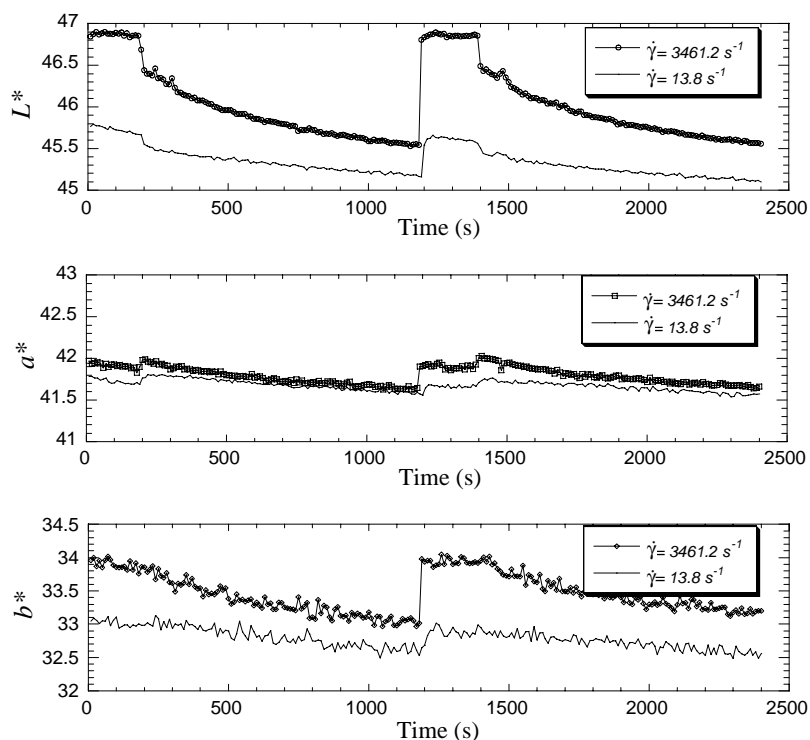


Fig. 4. The L^* , a^* and b^* measurement results for a red reference paint sample. A high shear ($\dot{\gamma} = 3461.2 \text{ s}^{-1}$) and a low shear ($\dot{\gamma} = 13.8 \text{ s}^{-1}$) were applied during the shearing period (0–200 and 1200–1400 s).

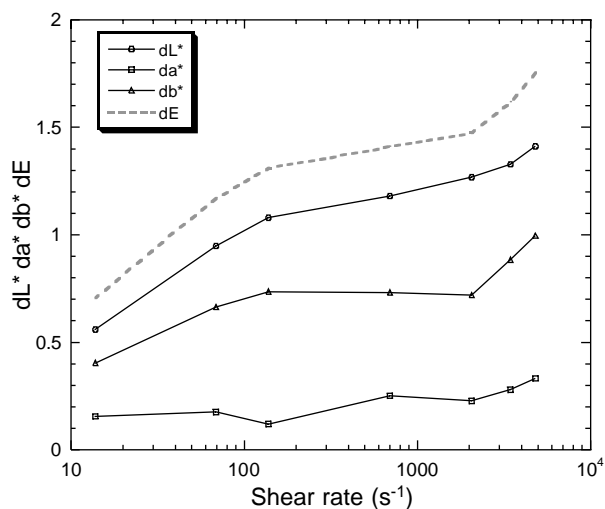


Fig. 5. The differences between the shearing and “quiescent” L^* , a^* and b^* values and also the overall colour difference dE plotted against applied shear rate.

results for two different millbase samples with a pre-shear rate of 3640.2 s^{-1} . Again, during the shearing periods, the colour values for both millbase samples appeared to remain roughly unchanged. On shear cessation, the MB120/47 sample showed a substantial increase in L^* value, and decreases in both a^* and b^* values. In addition, the magnitudes of difference between the shearing and relaxation values of the

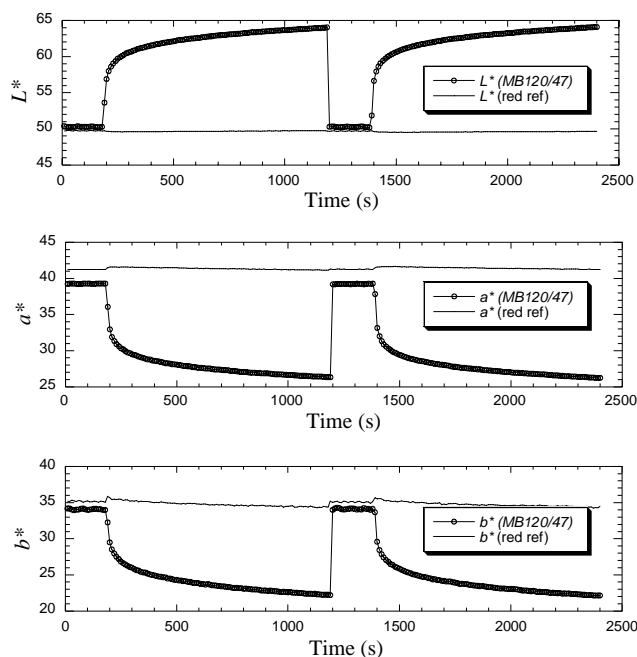


Fig. 6. The L^* , a^* and b^* measurement for the MB120/47 with a pre-shear ($\dot{\gamma} = 3640.2 \text{ s}^{-1}$) plotted with respect to time. The red reference sample measurement at the same condition was included for comparison.

MB120/47 sample were about 10 times greater than those previously measured for the red reference sample.

Although having the same composition, the “after shear colour relaxation” behaviour of the MB30/47 sample was very different. On the scale shown in Fig. 6, it appears that there is little or no change in colour for the MB30/47 during relaxation. This contrasts strikingly with the significant colour change in the MB120/47 case. The actual changes observed for the MB30/47 were of a comparable magnitude to the red reference sample but cannot be readily seen in Fig. 6.

2.4. Summary

From the colour measurement experiments carried out on the wet red reference and millbase paint samples, a number of findings can be summarised. During the relaxation period after shear cessation, the colour of both the red reference and millbase samples showed a tendency of gradual change. This progressive change with time reached a “quasi-equilibrium” state over roughly a period of 1000 s. However, the degree of change in paint colour was affected by the magnitude of the applied shear. As a result, the differences of the L^* , a^* and b^* values and the overall colour difference between the shearing and the quiescent values increase with increasing applied shear rate. From the measurement results on the millbase samples, not only can the colour values (L^* , a^* and b^*) of paint decrease with time on relaxation, they it can also increase. Also, even though the millbase samples had the same composition, the magnitude of colour change and the after-shear colour relaxation behaviour of the samples was significantly different.

The colour measurement technique developed in this study allowed the monitoring of the colour behaviour of the wet paint sample during and after shear. From the experimental findings, it was concluded that the colour change of the wet, red reference sample was associated with a change in certain aspect of paint microstructure. This quantity of microstructure has a tendency to change with time, and it gradually reached a quasi-equilibrium state after a certain time. The microstructure was influenced by shear and could relax to an equilibrium state after shear.

3. Direct optical observation of microstructure using the cambridge shearing system (CSS450)

3.1. Experimental apparatus, method, and protocol

A number of researchers have found that the colour properties of paint depend on the size and size distribution of the pigmented particles in the medium (Günther et al., 1989). Because of the opacity of paint, the pigment agglomerate size has in the past been examined by indirect methods such as light scattering tests (Mehta & Shah, 1982) or rheological measurement (Schröder, 1988). Others, such as Buttignol (1968) and Kaluza (1982) have carried out observations on the dry paint surface. Although these methods provide

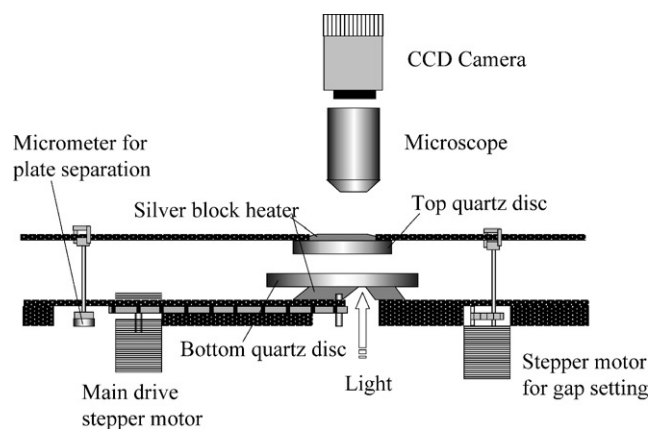


Fig. 7. Schematic diagram for the Cambridge shearing system showing the side view of this instrument.

information on the possible state of pigment dispersion, there is still very limited knowledge about the actual pigment dispersion of a wet flowing paint. Direct optical observation capable of showing the actual dispersion situation of a wet paint system was therefore required.

In this work, the direct optical observation on the wet paint sample was performed using a Linkam, Cambridge shearing system (CCS 450), which was initially developed by Mackley and co-workers at the University of Cambridge (Mackley et al., 1999). This system allows microstructure observation of test samples to be performed with shear induced flow under controlled conditions.

Fig. 7 schematically illustrates the components of the CCS450. The system consists of a computer controlled shear cell, where a parallel plate configuration formed by two quartz discs was used to contain the test sample. The bottom disc was driven by a stepper motor to generate either a constant speed or an oscillatory rotation. The top disc was attached to another stepper motor to adjust the gap width from 0 to 2500 μm . Both the circular motion and the gap width are controlled by the computer. The test temperature can be maintained using two silver block heating plates. By using a microscope and a CCD camera, the quasi-two dimensional images of the microstructure behaviour were observed and recorded during and after shear.

The paint sample was loaded onto the surface of the bottom disc, and the top disc was placed on the top to form a parallel-plate geometry. Due to the high opacity of the sample, a very narrow gap width of 10 μm was required. In addition, the intensity and the aperture of the light source for the microscope were adjusted to allow a sufficient light intensity for the observation. The paint sample was first sheared at 1000 s^{-1} for a hundred seconds to obtain a uniform initial state. After the cessation of shear, the pigment dispersion behaviour in paint sample was observed. Following a relaxation period of 1800 s, steady shears of 10, 100, and 1000 s^{-1} were applied. Each of these shearing period lasted for 30 s.

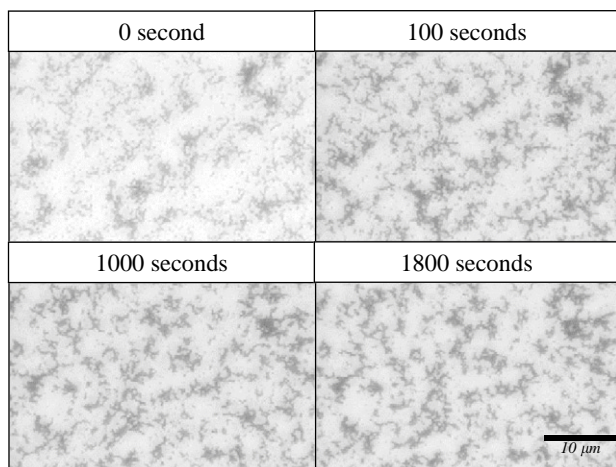


Fig. 8. Photographic image sequence obtained from the 10% thinner diluted red reference sample at 25°C after the cessation of pre-shear at 1000 s⁻¹.

3.2. Experimental observations

Preliminary observations were performed on the undiluted red reference paint sample. On shear cessation, the observed image was completely opaque, and the light from the microscope was unable to pass through the sample layer. This observation implied a uniform dispersed state of the pigment in the paint. With time, the pigment was seen to slowly form flocculated agglomerates, and this allowed light to pass through porous areas between flocculated agglomerates. Although qualitatively the flocculation of pigment was seen over time, it was impossible to quantify the flocculation from the observed image due to the heavily packed pigment agglomerates. Hence, the original red reference paint sample was diluted in order to obtain clearer images of optical observations. The original paint was diluted using both a resin solution and a thinner solvent to create two types of dilutions. The resin solution was prepared according to the recipe of the paint so that the ratio of resin to solvent equalled that of the original paint, while the thinner, provided by the manufacturer, is the same as that used in the original paint. The ratio of each dilution was made to be 10% (paint: diluting agent (thinner or resin solution) = 10:90) and 1% (Paint: diluting agent = 1:99) respectively.

In the optical observation for the 1% thinner diluted sample, the pigment agglomerates were found evenly dispersed in the suspension after the cessation of pre-shear. These small agglomerates were observed to undergo local Brownian motion such that the agglomerates vibrated randomly to collide with one another. However, this spontaneous vibration did not result in obvious flocculation of the pigment agglomerates.

In the observation carried out on the 10% thinner diluted sample shown in Fig. 8, partial flocculation of pigment agglomerates was observed immediately after shear cessation (0 s). During the relaxation period (100, 1000 s)

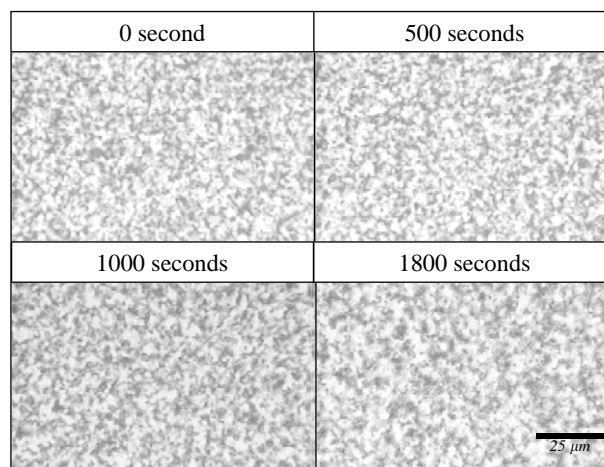


Fig. 9. Photographic image sequence obtained from a 10% resin diluted red reference sample at 25°C after the cessation of pre-shear at 1000 s⁻¹.

Brownian motion of the pigment agglomerates was observed. Agglomerates gradually flocculated with time, and the flocculation was found to occur when small sized pigment particles moved into contact with larger ones. As a result, the sizes of the pigment agglomerates slowly increased. After a period of roughly 1000 s, the system appeared to be relatively stable, and the sizes of the flocculated agglomerates did not show any further increase. When re-applying a high shear, these flocculated agglomerates were broken up again.

In terms of the optical observations on the resin diluted samples shown in Fig. 9, an obvious difference from previous cases was that the Brownian motion of the pigment was greatly reduced because of the matrix increased viscosity. In a similar way for the 10% resin diluted sample illustrated in Fig. 8, the pigment agglomerates were initially seen to uniformly disperse after the cessation of pre-shear. The pigment agglomerates exhibited slow Brownian movement, which resulted in a gradual flocculation of the pigment agglomerates during relaxation. The size of the pigment agglomerates was seen to increase slowly with time, but the rate of increase was much slower than that of the 10% thinner diluted sample. When re-applying shear, the flocculated agglomerates were broken up into smaller pieces, and the pigment dispersion resumed to its previous uniformly dispersed state after shear cessation.

3.3. Summary

From direct optical observation on the diluted systems of the red reference sample, it is clear that the paint pigment agglomerates undergo Brownian motion at all times, and the flocculation of paint pigment occurs after the cessation of shear. During the relaxation period, the flocculation of pigment results in an increase in agglomerate size. The flocculated pigment agglomerates can be broken up by an application of shear, where the resulting size and size

distribution of the pigment agglomerates is dependent on the magnitude of the shear. The flocculation and break-up mechanism of the pigment agglomerates has been seen in both thinner and resin diluted systems of the red reference sample, we assume this effect also occurs in the full concentration red reference sample.

The colour of red reference sample has been shown to have a progressive change during relaxation after shear, and the colour resumed its shearing value when the shear was re-applied. During optical observation, the size and, presumably, the size distribution of the pigment were seen to vary with time due to the flocculation, and the flocculation reached a “quasi-stable” state at roughly the same time as the colour during relaxation. The flocculated agglomerates could be broken up by shear, and the pigment dispersion retained its uniformly dispersed form. Clearly, the colour change behaviour of the wet paint can be associated with the variation in the size and size distribution of the pigment agglomerates. In addition, due to the fact that different milling times of the millbase samples can give rise to different size and size distribution of pigment agglomerates, it is expected that the different trends and magnitudes of the colour change observed using different millbase samples are probably determined by the initial size of their initial pigment particles.

4. Mathematical model for colour change of liquid paint

Work described previously has shown that colour change of certain wet paint is related to the modification of the pigment agglomerate size within the paint suspension. In order to correlate the microstructure behaviour (agglomerate size) of the pigment with the colour change of paint, a simple model has been developed.

4.1. Basis of model

A rigorous solution of the Maxwell equations has been derived by Mie (see Bohren & Huffman, 1983) to relate properties such as particle size, wavelength and the refractive index of spherical particles with particle scattering and absorption efficiencies. The Mie scattering theory permits insight into the relationship between colour properties and the size of pigment agglomerates. The theory is based on the scattering of one particle, and is generally applied to a dilute suspension system (Volz, 1995). A widely used formula in the field of Mie theory, given by Ven de Hulst (1957) can be expressed as

$$Q_{\text{ext}} = 2 - \frac{4}{\rho} \sin \rho + \frac{4}{\rho^2} (1 - \cos \rho), \quad (4)$$

where Q_{ext} is the extinction efficiency of the incident light passing through a homogeneous media containing scattering particles. The term ρ is the phase lag having the relationship $\rho = 2\pi D(m - 1)/\lambda$, where D represents particle diameter, m the ratio of refractive indices of pigment to the media, and

λ the wavelength of light. This equation is valid for back scatter at 0° to the incident beam (Ven de Hulst, 1957).

The above equation links the extinction efficiency of scattered light to the particle diameter D . In order to correlate the colour of pigmented suspension with its pigment size, a simple model has been developed. The model makes a number of key simplifying assumptions. Firstly, it was assumed that Mie scattering is the governing physical mechanism for the scattering behaviour of light from the paint suspension. Particles obeying Mie theory are assumed to be non-absorbing and spherical. The suspension is assumed to be dilute and that the distance between particles is assumed to be greater than the diameter of the particle itself. In addition, the size of the pigment agglomerate is assumed to be mono-disperse, and can be characterised by a single particle diameter, D . All of these assumptions are not necessarily true and Mie scattering is unlikely to be the sole scattering mechanism. The scattering particles are non spherical and have a high concentration. In addition, the particles are polydisperse in size.

A further key assumption is necessary in order to link Mie scattering to reflectance at a specific wavelength. For a given mean particle size D_0 , it is possible, using Eq. (4), to evaluate a Mie scattering extinction efficiency $Q_{\text{ext}D_0}(\lambda)$. This value will change for different wavelengths. It is also possible to experimentally measure the experimental reflectance response for a sample with a mean particle size, D_0 . This again will be a function of wavelength and is designated as $R_{D_0}(\lambda)$.

If the particle size changes from D_0 to D_i , from Eq. (4) a new scattering extinction efficiency can be computed as $Q_{\text{ext}D_i}(\lambda)$. We have assumed that at any given wavelength the ratio of the scattering efficiencies $Q_{\text{ext}D_i}(\lambda)/Q_{\text{ext}D_0}(\lambda)$ is equal to the ratio of the reflection coefficients $R_{D_i}(\lambda)/R_{D_0}(\lambda)$ such that

$$\frac{Q_{\text{ext}D_i}(\lambda)}{Q_{\text{ext}D_0}(\lambda)} = \frac{R_{D_i}(\lambda)}{R_{D_0}(\lambda)} \quad (5)$$

if D_0 and D_i are known, $Q_{\text{ext}D_0}(\lambda)$ and $Q_{\text{ext}D_i}(\lambda)$ can be computed from Eq. (4). If $R_{D_0}(\lambda)$ is experimentally measured, Eq. (5) can then be used to predict the values of $R_{D_i}(\lambda)$ at a different value of D . Having evaluated $R_{D_i}(\lambda)$ from Eq. (5), new values of the L^* , a^* and b^* corresponding to this reflectance characteristic can be evaluated.

4.2. Modelling procedure

The modelling procedure is illustrated in Fig. 10. Based on the above assumptions, a reference condition corresponding to the state of shear cessation was specified, where the size of the pigment agglomerate was set to be D_0 . A test condition after t seconds of shear relaxation was also specified, and the corresponding pigment size in this condition was set to be D_i . The size of pigment agglomerates has been observed to grow after shear cessation. Hence, the size of the pigment

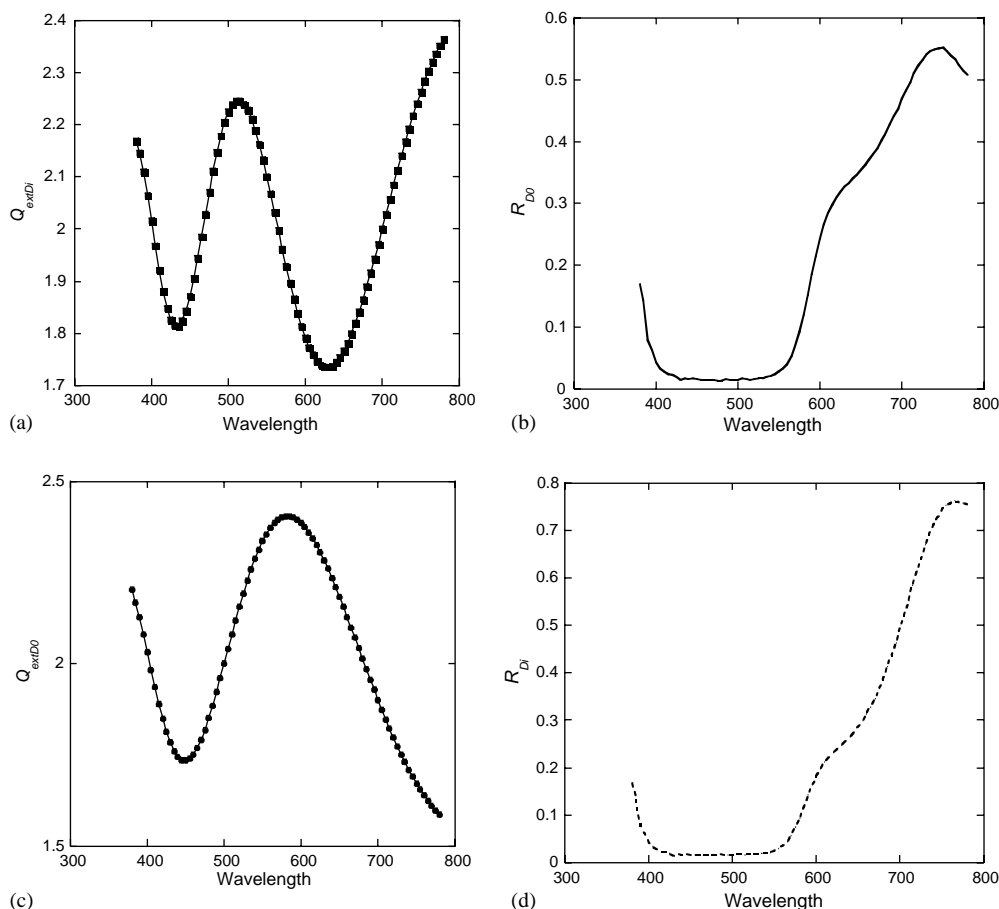


Fig. 10. Example of the modelling procedure: (a) mie scattering extinction efficiency $Q_{\text{ext}D_0}(\lambda)$ computed for reference D_0 using Eq. (4), (b) experimental measurement of reflectance $R_{D_0}(\lambda)$ for the reference condition with $D = D_0$, (c) Mie scattering extinction efficiency $Q_{\text{ext}D_i}(\lambda)$ for a particle size of D_i as calculated using Eq. (4) and (d) reflectance $R_{D_i}(\lambda)$ calculated using Eq. (5) for a range of λ . Data in (b) can then be converted into L^* , a^* and b^* values for this appropriate particle size.

agglomerates increased from D_0 to D_i after t seconds of relaxation.

In Fig. 10(a) and (c), the extinction efficiency factors calculated from Eq. (4) at diameters D_0 and D_i , are shown respectively. Both $Q_{\text{ext}D_i}(\lambda)$ and $Q_{\text{ext}D_0}(\lambda)$ were obtained using Eq. (4) from a knowledge of D_0 and D_i , respectively. The experimentally obtained reflectance spectrum of the red reference sample at the reference condition ($R_{D_0}(\lambda)$) is also shown in Fig. 10(b). From a knowledge of the ratios of the extinction efficiency at each diameter, it was then possible, by using Eq. (5), and the reference reflectivity data in Fig. 10(b), to compute the reflectance spectrum for the test condition, $R_{D_i}(\lambda)$, and this is shown in Fig. 10(d).

The reflectance spectra obtained in 10(d) can readily be converted to L^* , a^* and b^* colour values using Eqs. (1) and (2) and by repeating the procedure for different values of D_i it is possible to build up a graph of the predicted L^* , a^* and b^* colour values for different particle sizes. This data is shown in Fig. 11 and illustrates the way L^* , a^* and b^* values are predicted to change from the reference state as the particle size changes.

4.3. A case study

In order to rank this model with experimental results, a case study was performed using the experimental result on a 10% resin diluted red reference sample. From its colour measurement experiment, the reflectance spectrum was measured immediately after shear cessation. The pre-dominant size of pigment agglomerate at this state, determined from the image obtained using direct optical observation, was set to be 2.2 μm . After 1000 s of relaxation, this pre-dominant size changed to 2.5 μm . The ratio of the refractive index of the pigment and the media was estimated to be 2.5. Using the above parameters, the procedure of the model was performed over a size range from 0.1 to 3.0 μm using a *Mathematica*TM program. The resultant L^* , a^* and b^* values as functions of pigment diameter are plotted in Fig. 11.

Table 1 shows the result of the case study and its corresponding colour measurement results. The predicted L^* , a^* and b^* values for pigment diameters from 2.2 μm to roughly 2.5 μm showed similar trends to the behaviour seen in the colour measurement experiment. For example, both the L^*

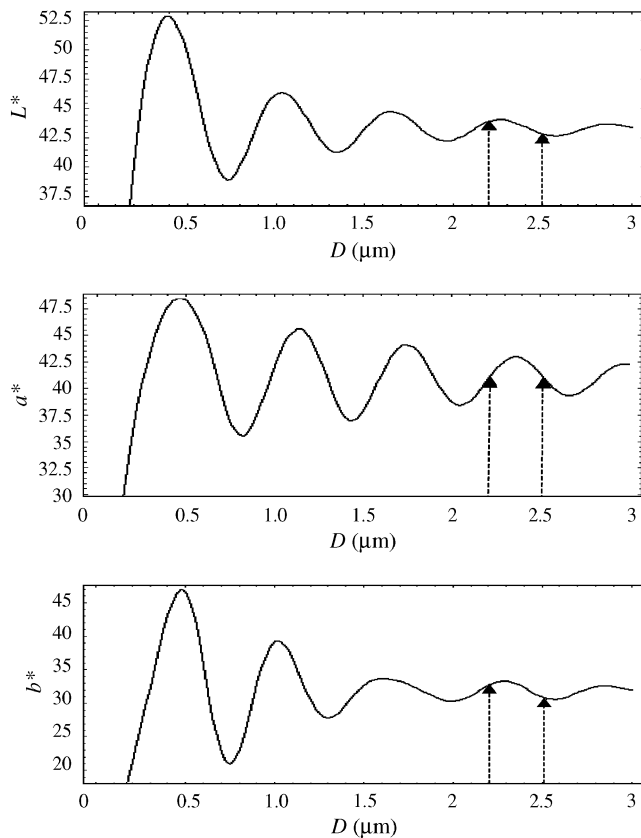


Fig. 11. The L^* , a^* and b^* values plotted with respect to the particle diameter calculated using the proposed model, where the reference diameter used was $2.2 \mu\text{m}$. The arrows indicates the range size change for the case study.

and b^* values over this size range gradually decreased with increasing size, and the values at $2.5 \mu\text{m}$ resembled those obtained experimentally after a period of relaxation. For the a^* , the colour value increased initially then decreased with increasing size, and the value at both 2.2 and $2.5 \mu\text{m}$ were similar to those obtained from the experiment. Because the size of pigment agglomerates in the paint was expected to increase during the relaxation period, it was clear that the general trend of the model prediction agreed well with the experimental result.

Table 1

A set of L^* , a^* and b^* values obtained from the colour measurement experiment on a 10% resin diluted red reference sample both during shear and after shear relaxation. The results were compared with model predictions for particle diameters changing from 2.2 to $2.5 \mu\text{m}$

| | Colour Measurement | | Modelling Prediction | |
|-------------------|------------------------|------------------------|----------------------|-------------------|
| | During shear | After relaxation | Reference condition | Test condition |
| L^* | 44.0 | 42.5 | 44.0 | 42.6 |
| a^* | 41.3 | 41.0 | 41.3 | 41.2 |
| b^* | 33.0 | 31.5 | 33.0 | 31 |
| Particle diameter | $\sim 2.2 \mu\text{m}$ | $\sim 2.5 \mu\text{m}$ | $2.2 \mu\text{m}$ | $2.5 \mu\text{m}$ |

Fig. 11 shows that the trend of colour change depends on the initial size of pigment, where L^* , a^* and b^* values may increase or decrease with increasing particle diameter. Also, the values at smaller size range showed larger variations in magnitude with increasing size. This can qualitatively explain the colour change behaviour seen for the millbase sample, where at long milling time, small pigment size resulted; hence, a large, distinctive colour change pattern occurred.

In reality, the actual pigment has a size distribution and the exact pigment agglomerate size could not be measured. In addition, the scattering by concentrated pigment particles with a size distribution will be far more complicated than the modelling presented here. However, through this case study, it can be seen that the model is capable of giving a qualitative or semi-quantitative prediction to the colour change behaviour of paint. This model also demonstrates that an increase in particle size during relaxation can lead to either increases or decreases in L^* , a^* and b^* values depending on the initial particle size.

5. Conclusions

A novel, in situ colour measurement experimental technique was successfully developed to allow direct colour monitoring of flowing wet paint when subjected to shear. In addition, direct optical observation was carried out to study the microstructure evolution of pigment agglomerates in a paint suspension. The pigment in paint shows a natural tendency to flocculate, and the flocculated agglomerates in the suspension can be broken up into smaller sizes by an applied shear stress. Hence, the colour of wet paint shows a progressive change with time during relaxation, and the degree of colour change depends on the magnitude of applied shear and also the time duration after shear. In order to achieve an understanding to this complex problem, the colour change behaviour of paint was modelled. Although the assumptions made for this model are highly simplified, the model was capable of showing a qualitative, and in some

cases, a semi-quantitative consistency with the experimental findings.

Notation

| | |
|--|--|
| D_0 | particle diameter at reference condition |
| D_i | particle diameter at test condition |
| L^*, a^*, b^* | colour values from CIELAB colour formula |
| m | ratio of refractive indices of pigment over media |
| $R_{D_0}(\lambda)$ | reflectance spectrum at reference condition |
| $R_{D_i}(\lambda)$ | reflectance spectrum at test condition |
| Q_{ext} | extinction efficiency |
| $Q_{\text{ext}D_0}(\lambda)$ | extinction efficiency at particle size D_0 |
| $Q_{\text{ext}D_i}(\lambda)$ | extinction efficiency at particle size D_i |
| X, Y, Z | imaginary primaries from the CIE colour system |
| X_n, Y_n, Z_n | imaginary primaries for a perfect white surface |
| $\bar{x}(\lambda), \bar{y}(\lambda), \bar{z}(\lambda)$ | colour matching functions of the CIE colour system |
| λ | wavelength of incidence |
| ρ | phase lag defined by Eq. (4) |

Abbreviations

| | |
|--------|---------------------------------------|
| CCS450 | cambridge shearing system |
| CIE | international commission of luminance |
| MPR | multi-pass rheometer |

Acknowledgements

The authors would like to thank ICI AUTOCOLOR (now PPG Industries UK Ltd.) for their technical and financial

support. YKC also wishes to thank the Cambridge Overseas Trust and Queens' College for their financial support. We would also like to thank Cambridge Reactor Design (CRD) for test cell manufacture, Eland Test Plant Ltd and Linkam Scientific for technical support.

References

- Blakey, R. R. (1989). Paint quality control via flocculation measurement. *Pigments*, 174-4127, 664–666.
- Bohren, C. F., & Huffman, D. R. (1983). *Absorption and scattering of light by small particles*. New York: Wiley-Interscience.
- Buttignol, V. (1968). Optical behavior of iron oxide pigments. *Journal of Paint Technology*, 40-526, 480–493.
- Günthert, P., Hauser, P., & Radtke, V. (1989). Effect of pigment particle size on application properties. *Rev. Prog. Coloration*, 19, 41–48.
- Hotter, H. C., Sarofim, A. F., Dalzell, W. H., & Vasalos, I. A. (1971). Optical properties of coatings. Effect of pigment concentration. *AIAA Journal*, 9-10, 1895–1898.
- Hunt, R. W. G. (2002). *Measuring colour* (4th ed.). Fountain Press Ltd.
- Kalau, U. (1982). Flocculation of pigment in paints—effects and causes. *Progress in Organic Coatings*, 10, 289–330.
- Mackley, M. R., Marshall, R. T. J., & Smeulders, J. B. A. F. (1995). The multipass rheometer. *Journal of Rheology*, 39(6), 1293–1309.
- Mackley, M. R., Wannaborworn, S., Gao, P., & Zhao, F. (1999). The optical microscopy of sheared liquids using a newly developed optical stage. *Microscopy and Analysis*, 69, 25–29.
- McDonald, R. (1997). *Colour physics for industries* (2nd ed.). Society of Dyers and Colourists.
- Mehta, K. T., & Shah, H. S. (1982). Particle size determination through spectral transmission measurement: A critical survey. *Journal of Scientific and Industrial Research*, 41-05, 292–299.
- Schröder, J. (1988). Methods of determining the state of pigment dispersion. *Progress in Organic Coatings*, 15, 337–353.
- Ven de Hulst, H. C. (1957). *Light scattering by small particles*. London: Wiley.
- Volz, H. G. (1995). *Industrial color testing fundamentals and techniques*. Weinheim: VCH.
- Wee, W. -K., & Mackley, M. R. (1998). The rheology and process of a concentrated cellulose acetate solution. *Chemical Engineering Science*, 53(6), 1131–1144.
- Wyszecki, G., & Stiles, W. S. (1982). *Color science: Concepts and methods, quantitative data and formulae* (2nd ed.). New York: Wiley.